Laboratori Nazionali di Frascati

LNF-68/23

M. Grilli et al. : POSITIVE-PION PHOTOPRODUCTION BY LINEARLY POLARIZED GAMMA RAYS. - I. EXPERIMENTAL METHOD AND RESULTS.

Estratto da : Nuovo Cimento 54A, 877 (1968)

M. GRILLI, *et al.*
21 Aprile 1968
Il Nuovo Cimento
Serie X, Vol. 54 A, pag. 877-896

Positive-Pion Photoproduction by Linearly Polarized γ Rays.

I. - Experimental Method and Results.

M. GRILLI, P. SPILLANTINI and F. SOSO
Laboratori Nazionali di Frascati del CNEN - Roma

M. NIGRO, E. SCHIAVUTA and V. VALENTE
Istituto di Fisica dell'Università - Padova
Istituto Nazionale di Fisica Nucleare - Sezione di Padova

(ricevuto il 10 Ottobre 1967)

Summary. — The apparatus and the experimental method used for the measurements of the single-π^+ photoproduction by linearly polarized γ rays are described. The present results on the asymmetry ratio $A(\theta)$ are summaized. The range covered by our results is $\theta = (30 \div 145)°$ (c.m.) and $E_\gamma = (200 \div 450)$ MeV.

Introduction.

Linearly polarized photon beams make it possible to study some aspects of positive-pion photoproduction that are not explicitly revealed in experiments involving unpolarized photons. In particular, the quantities $\sigma_\perp(\theta)$ and $\sigma_\parallel(\theta)$ can be determined separately, where $\sigma_\perp(\theta)(\sigma_\parallel(\theta))$ is the differential cross-section for producing a pion in a plane perpendicular (parallel) to the polarization plane of the incident photon. As the «retardation term» in π^+ photoproduction contributes only to $\sigma_\parallel$, the $\sigma_\perp$ is particularly suitable for a phenomenological theoretical analysis of the photoproduction process.

The complementarity of measurements by polarized and unpolarized γ' rays has been extensively discussed in many theoretical ([1-5]) and experimental papers ([6]).

([1]) A. DONNACHIE and G. SHOW: *Ann. of Phys.*, **37**, 333 (1966).
([2]) W. SCHMIDT: *Zeits. Phys.*, **182**, 76 (1964).
([3]) G. T. HOFF *Phys. Rev.*, **122**, 665 1961).
([4]) M. GOURDIN and PH. SALIN: *Nuovo Cimento*, **27**, 193 (1963).
([5]) M. NIGRO and E. SCHIAVUTA: *Nuovo Cimento*, **50**, 358 (1967).
([6]) R. C. SMITH and R. F. MOZLEY: *Phys. Rev.*, **130**, 2429 (1963).

The experiment described below consisted of a measurement of the asymmetry ratio $A(\theta) = (\sigma_\perp(\theta) - \sigma_\parallel(\theta))/(\sigma_\perp(\theta) + \sigma_\parallel(\theta))$ as a function of pion angle (c.m.) $(\theta = (30° \div 145°))$ for several photon energies $(E_\gamma = (200 \div 450)$ MeV), for the process

$$\gamma + p = n + \pi^+ . \tag{1}$$

Part of the results of these measurements has been previously published; precisely that for $E_\gamma = (200 \div 250)$ MeV (7), and at $\theta = 90°$ for $E_\gamma = (200 \div 450)$ MeV (8).

In the present work we report more details on the features of γ's polarized beam (Sect. 1), on the apparatus (Sect. 2) and on the logic of the experiment (Sect. 3). In Sect. 4 we give, finally, a summary of the results.

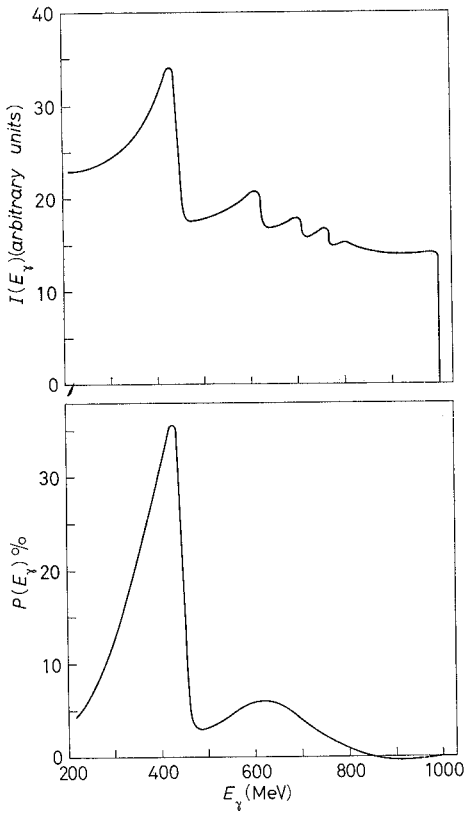

Fig. 1. – A theoretical intensity and polarization spectrum in the case of coherent bremsstrahlung from 1 GeV electrons in a single diamond crystal (9). $\Phi = 13.26°$, $\Theta = 46.50$ mrad, angular divergence of the beam = 0.704 mrad.

1. – Characteristics of the beam.

The polarized γ'-ray beam was produced by the interaction of 1 GeV electrons, of the Frascati electron-synchrotron, in a single diamond crystal by means of the well-known process of coherent bremsstrahlung. This beam has has been prepared by BARBIELLINI, BOLOGNA, DIAMBRINI, MURTAS (9).

The characteristics of the beam are determined by the angle Θ be-

(7) P. GORENSTEIN, M. GRILLI, P. SPILLANTINI, M. NIGRO, E. SCHIAVUTA, F. SOSO and V. VALENTE: *Phys. Lett.*, **19**, 157 (1965).

(8) P. GORENSTEIN, M. GRILLI, F. SOSO, P. SPILLANTINI, M. NIGRO, E. SCHIAVUTA and V. VALENTE: *Phys. Lett.*, **23**, 394 (1966).

(9) G. BARBIELLINI, G. BOLOGNA, G. DIAMBRINI and G. P. MURTAS: *Phys. Rev. Lett.*, **8**, 112 (1962).

tween the incident electron direction, $\overline{p}_e$, and the (1 1 0) axis of the crystal and by the angle Φ between the planes $[\overline{p}_e, (1\,1\,0)]$ and $[(1\,1\,0), (0\,0\,1)]$. As is known, in comparison to the bremsstrahlung beam from an amorphous target there is an enhancement of the intensity in the neighbourhood of certain γ-ray energies. The position (E_{peak}) of the « principal » maximum (the first maximum) can be varied by suitable adjustment of the angle Θ. In the region of this maximum the γ rays are linearly polarized.

Typical theoretical intensity and polarization curves are shown in Fig. 1.

In the following we will not discuss the features of such spectra but essentially the procedure and some precautions to use in order to work with a coherent beam, which involves several peculiar difficulties.

A large part of these procedures has been developed by BARBIELLINI *et al.* [9].

1·1. *Geometrical alignment of the crystal.* – During this operation great care has been applied in order to shield against possible sources of incoherent radiation from the crystal support, as these sources would reduce the coherence of the accepted spectrum.

1·2. *Search of « zero position » of the crystal.* – The search of the « zero position » of the crystal, *i.e.* the position $\Phi = \Theta = 0$, is a very critical operation because an error $\Delta\Theta = 1'$ would shift E_{peak} by ~ 4 MeV. Moreover a similar error on Θ or Φ would give a variation of photon intensity, in the accepted energy band, of $\sim 2\,\%$ (the corresponding polarization would vary only by less than 0.01).

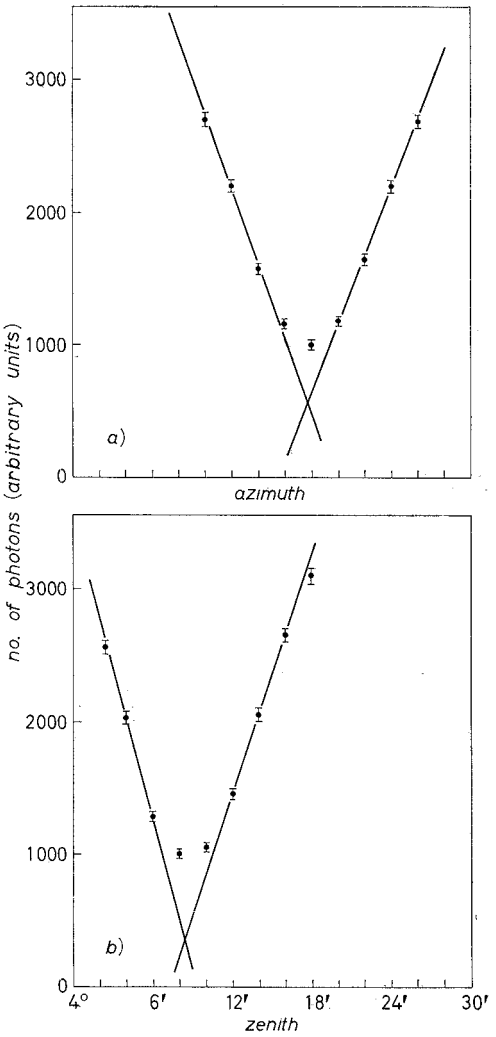

Fig. 2. – An example of the procedure to follow for searching the « zero position » of the crystal. *a*) 300 MeV, Zenith = 4° 8'; *b*) $E = 300$ MeV, Azimuth = 4° 17' 35".

The « zero position » of the crystal was determined by searching a minimum on the number of photons contained in a narrow energy band (Fig. 2). The precision obtainable on the « zero position » is of the order of $\Delta\Phi = \Delta\Theta = \pm 0.5'$.

1·3. *The intensity spectrum and the polarization of the beam.* – Actually the precision we obtained on photon intensity was better than that corresponding to the indicated precision on « zero position » (see Fig. 2). In fact, the photon-

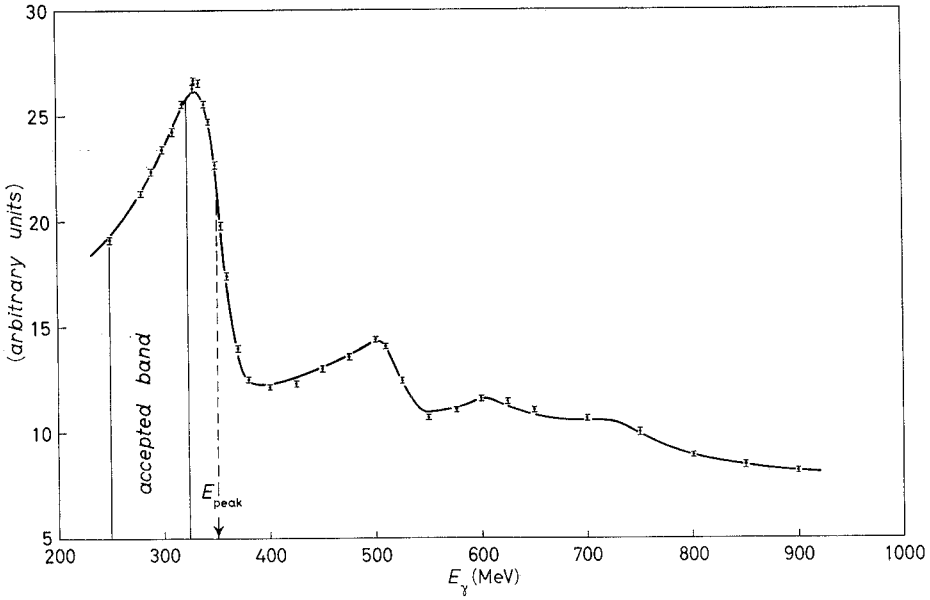

Fig. 3. – Comparison between a measured and the expected intensity spectrum. $\Phi = 13.26°$, $\Theta = 31.13$ mrad, angular divergence of the beam = 0.704 mrad. • Experimental points, ——— expected spectrum.

intensity spectrum was measured simultaneously with great detail, during the π^+ measurements, by means of a pair spectrometer, (see Fig. 4) and was required to reproduce accurately (within 0.3 %) the expected spectrum (see Fig. 3).

This spectrum has been obtained (*) from the theoretical spectrum (see Fig. 1) by including the following effects:

a) angular divergence of the primary beam of the electrons,

b) multiple scattering of the electrons into the crystal,

(*) G. BOLOGNA: private communication. More details on these calculations will be found in a forthcoming paper by this author on this subject.

c) angular divergence of photon's beam (about 0.7 mrad in our experiment),

d) finite resolution of pair spectrometer ($\Delta E_\gamma/E_\gamma = \pm 4\,\%$).

The agreement required between the measured and expected spectra limits the error in the polarization (*), calculated with the same procedure (*), to less than $\Delta P = \pm 0.005$. By combining this precision with possible errors coming from crystal's alignment we estimate a total error in P certainly smaller than $\Delta P = \pm 0.01$.

Experimental checks of these calculations on P have been done at Frascati ([10,11]) and Desy ([12]).

2. – Experimental apparatus.

2·1. – A general view of all the experimental apparatus is reported in Fig. 4.

Positive pions, produced at a certain angle θ_1 (lab) were detected and identified by a system consisting of a strong focusing magnet and a counter telescope (see Fig. 5).

The magnet has been extensively described by ([13,14]). The principal characteristics of it are summarized in Table I. The total momentum acceptance was $\Delta p/p = 0.25$ with a slowly varying solid angle over that region of acceptance of about $5 \cdot 10^{-3}$ sr. By means of a three-unit counter system (*A*, *B*, *C*

TABLE I. – *Parameters of the magnet.*

Source-magnet distance	$S_0 = 31$ cm
Image-magnet distance	$d = 51.6$ cm
Total distance source-image	$S = 261$ cm
Linear magnification (horizontal)	$M_h = 0.2$
Linear magnification (vertical)	$M_v = 6$
Dispersion (at the image position)	$D = 0.03$ cm^{-1}

(*) For the definition of this quantity see formula (4) (Sect. **3**).

([10]) G. BARBIELLINI, G. BOLOGNA, G. DIAMBRINI and G. P. MURTAS: *Phys. Rev. Lett.*, **9**, 9 (1962).

([11]) G. BARBIELLINI, F. GRIANTI, T. LETARDI and R. VISENTIN: *Nuovo Cimento*, (in press).

([12]) L. CRIEGEE, G. LUTZ, H. D. SCHULZ, U. TIMM and W. ZIMMERMANN: *Phys. Rev. Lett.*, **16**, 1031 (1966).

([13]) G. SACERDOTI and L. TAU: *Nucl. Instr. and Meth.*, **16**, 139 (1962).

([14]) B. BORGIA, P. JOOS and M. GRILLI: Internal Report LNF-66/15 (1966).

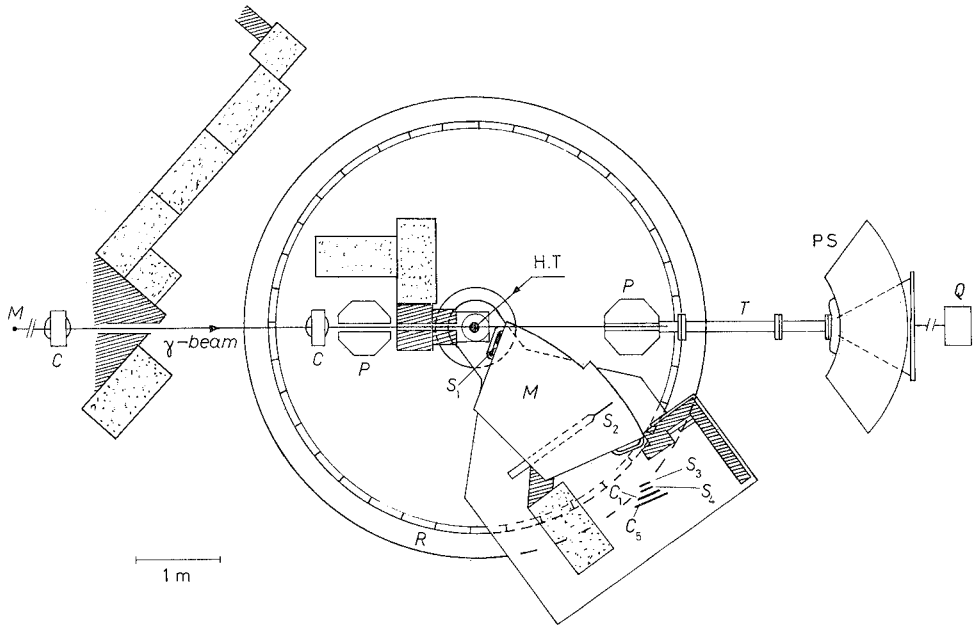

Fig. 4. – A general view of experimental apparatus: C: collimators; P: sweeping magnet; $H.T.$: liquid hydrogen target; M: magnetic spectrometer; Q: quantameter (Wilson's type); $S_1 \ldots S_5$: plastic scintillators; C_1: Čerenkov counter; ▦ concrete; ▨ Pb.

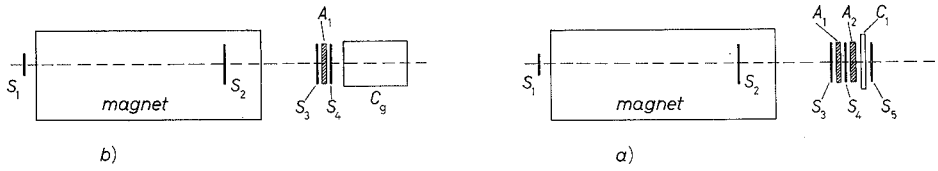

Fig. 5. – Counter's telescope (not to scale): *a*) telescope for « low-energy » pions ($p < 200$ MeV/c); *b*) telescope for « high-energy » pions ($p > 200$ MeV/c). $S_1 \ldots S_5$: plastic scintillators; C_1: plexiglass Čerenkov; C: gas Čerenkov (CO_2); $A_{1,2}$: absorber (Cu).

in Fig. 6), located in the focal plane, the total momentum acceptance was divided in eight momentum channels.

Standard techniques were used to select the pions among the other particles. Protons did not have sufficient range to reach S_4. The electrons entering the spectrometer were largely eliminated by either or both of two veto counters: C_1 and S_5 (see Fig. 5*a*)). The electrons but not pions would produce Čerenkov radiation in C_1. The counter S_5 would be reached by surviving electrons while the pions were stopped, for $p < 200$ MeV/c (« Low-energy pions »), in the ab-

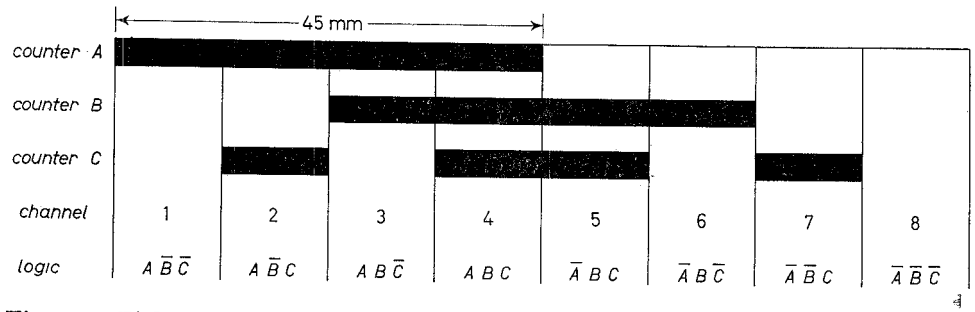

Fig. 6. – Eight-momentum-channel system. The tree counters A, B, C are indicated as a unique counter S_3 in Fig. 5.

sorber A_2. In the measurement of π with higher momentum ($p > 200$ MeV/c) (see Fig. 5*b*)) we have used a gas Čerenkov counter [C_4; CO_2; $(5 \div 7)$ atm] to reject the electrons. In either case the rejection efficiency against the electrons was $\sim 95\,\%$.

2·2. – The block diagram of the system used to identify the π^+ (in the case $p > 200$ MeV/c) is shown in Fig. 7.

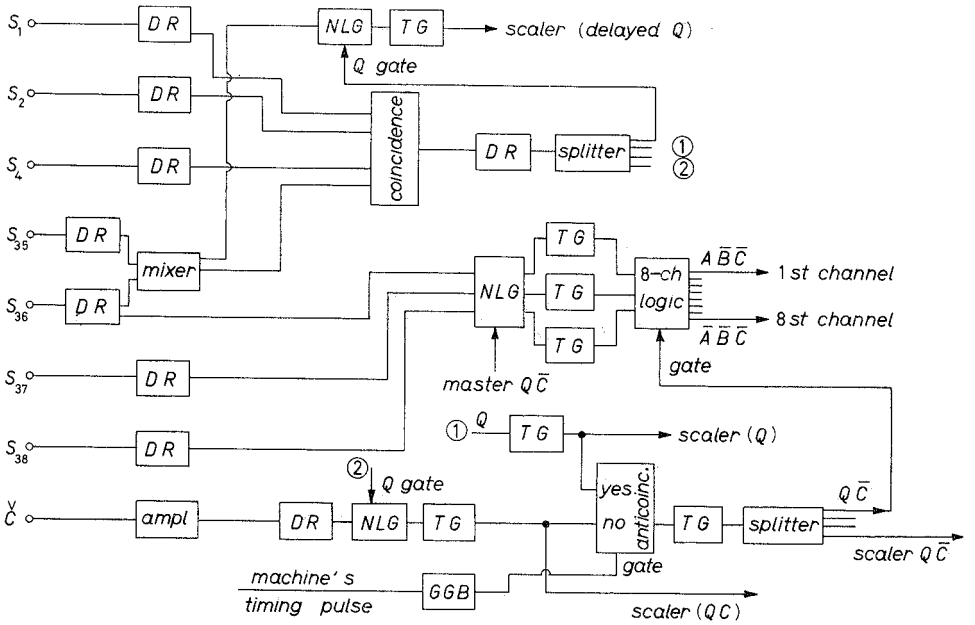

Fig. 7. – Electronics block diagram: AMP: amplifier; DR: fast discriminator and shaper; NLG: nonlinear gate; TG: triger; GGB: beam synchronized gate.

A first coincidence

$$Q = S_1 S_2 S_3 S_4$$

defines particles (pions and electrons) of the right momentum, which traverse the telescope. The Čerenkov counter signal (gated by Q) in coincidence with $Q(QC)$ or in anticoincidence ($Q\bar{C}$) separates the electrons from the pions. Figure 8 shows the efficiency curve of this counter.

The « master » $Q\bar{C}$ is used to gate the signals of the counters S_{26}, S_{37}, S_{38}. (A, B, C, respectively, in Fig. 6). A 8-channel logic circuit (8-CH LOGIC in Fig. 7) makes the correlations $A\bar{B}\bar{C}$, ... $\bar{A}\bar{B}\bar{C}$, indicated in Fig. 6.

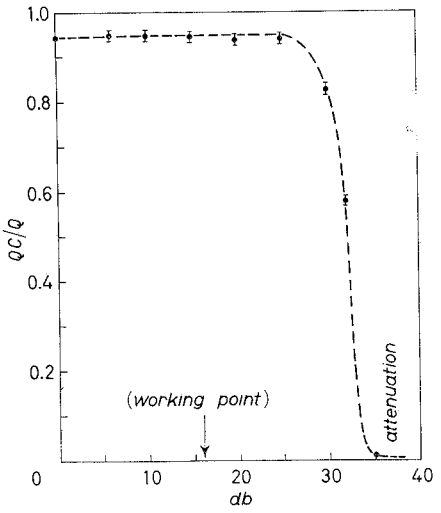

Fig. 8. – Efficiency curve for the gas Čerenkov. The measurement of this effciency was made with the same geometry used during the experiment (beam's divergence at the Čerenkov ($\delta \sim \pm 6°$)). The efficiency of this Čerenkov for a « parallel » beam ($\delta = \pm 3°$) of electrons was better than 99%. $\theta_i = 0°$, $p = 300$ MeV/c, $P = 5$ atm.

3. – Experimental method.

3·1. – We have measured the asymmetry ratio

$$A(\theta, E_\gamma) = \frac{\sigma_\perp(\theta, E_\gamma) - \sigma_\parallel(\theta, E_\gamma)}{\sigma_\perp(\theta, E_\gamma) + \sigma_\parallel(\theta, E_\gamma)}, \tag{2}$$

starting from the observed pion yield (C_+, C_-) by means of the relation

$$A(\theta, E_\gamma) = \frac{1}{P} \frac{\left(C_+(\theta, E_\gamma) - B_+(\theta, E_\gamma)\right) - \left(C_-(\theta, E_\gamma) - B_-(\theta, E_\gamma)\right)}{C_+(\theta, E_\gamma) - B_+(\theta, E_\gamma) + C_-(\theta, E_\gamma) - B_-(\theta, E_\gamma)}, \tag{3}$$

where

$$P = \frac{N_\perp - N_\parallel}{N_\perp + N_\parallel} \tag{4}$$

is the beam polarization.

$N_\perp(N_\parallel)$ is the relative number of photons having their electric vector perpendicular (parallel) to the (γ, π) plane.

The quantities $\sigma_\perp(\theta, E_\gamma)$, $[\sigma_\parallel(\theta, E_\gamma)]$ have been previously defined (see « Introduction »).

The other quantities entering (3) are:

a) $C_+(\theta, E_\gamma)\,[C_-(\theta, E_\gamma)]$ total yield of pions, in the accepted momentum band and for a given angle θ, for a fixed number of incident photons in a narrow energy band around E_γ, when $P>0$ $(P<0)$.

b) $B_+(\theta, E_\gamma)$ $[B-(\theta, E_\gamma)]$ background events in process (1), measured under the same conditions as the corresponding C_+ [and C_-].

The kinematical conditions (E_γ, θ) were fixed by measuring the pions at a fixed angle and momentum in the laboratory system (θ_l, p).

The cross section $\sigma_\perp$ and $\sigma_\parallel$ are related to the observed counting rates as follows:

$$(5) \qquad C_\pm - B_\pm = K(\sigma_\perp N_\perp + \sigma_\parallel N_\parallel) = \frac{K}{2}(N_\perp + N_\parallel)(\sigma_\perp + \sigma_\parallel)[1 \pm |P| A]\,,$$

where the proportionality constant K, depending on target size, solid angle, etc., is the same for both signs of beam polarization.

From the relation (5) we obtain (3) assuming that the absolute value of the polarization P, and the total number of photons in the accepted energy band, $(N_\perp + N_\parallel)$, are the same for the two cases C_+ or C_-.

We have obtained, during the experiment, this equality of $|P|$ and of the photon intensity by requiring that the two γ-ray intensity spectra simultaneously measured in the case $P>0$ and $P<0$ agree better than 0.5 % (see Fig. 9).

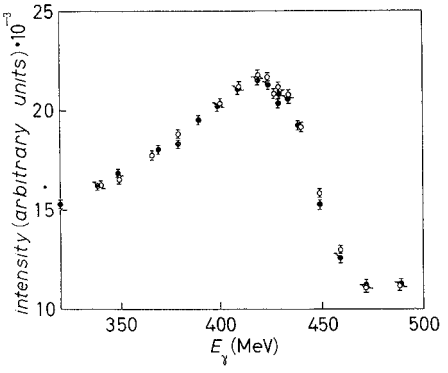

Fig. 9. – A comparison between two experimental intensity spectra relative to the cases $P>0$ (o) and $P<0$ (•).

Actually, during our measurements we have used, for experimental convenience, not a single diamond crystal but two different crystals in order to obtain the two signs of beam polarization. Both the zero position and the photon spectrum of these two crystals were accurately and continuously checked, as we have said, by means of the pair spectrometer. These crystals could be inserted or taken out without any change in their zero position and

TABLE II.

Date		$S35$	$P\chi^2$	χ^2	Skewness	$S36$	$P\chi^2$	χ^2	Skewness	$S37$	$P\chi^2$	χ^2	Skewness	No. of pions	
														$S35$	$S36$
1	2	3	4	5	6	7	8	9	10	11	12	13	14	15	16
1810	1	11	0.668	5.82	0.795	13	0.434	10.09	−0.453	10	0.295	8.46	0.494	10 787	7 162
1810	2	18	0.968	6.64	−0.154	19	0.581	14.25	0.930	17	0.478	13.63	0.240	14 654	8 971
1810	1+2	29	0.964	12.46	0.414	32	0.558	24.34	0.263	27	0.395	22.10	0.333	25 441	16 133
1012	1	32	0.787	21.91	−0.821	36	0.004	58.21	0.240	32	0.807	21.46	0.300	25 899	17 650
1012	2	38	0.635	30.63	−0.279	39	0.507	34.22	−0.122	38	0.460	34.17	−0.508	20 147	13 857
1012	1+2	70	0.800	52.54	−0.545	75	0.023	92.42	0.165	70	0.704	55.63	−0.268	46 046	31 507
1303	1	30	0.187	33.33	0.032	30	0.113	36.13	0.448	30	0.065	38.96	0.078	20 166	12 805
1303	2	32	0.861	20.98	−0.403	32	0.449	29.32	−0.599	32	0.325	31.91	0.200	18 948	11 951
1303	1+2	62	0.540	54.31	−0.107	62	0.183	65.45	0.030	62	0.088	70.87	0.131	39 114	24 756
604	1	21	0.548	18.62	0.270	21	0.070	30.08	−0.608	21	0.331	22.20	−0.084	4 189	1 795
604	2	14	0.013	27.10	0.094	14	0.410	13.51	0.167	14	0.996	3.64	0.800	4 254	1 865
604	1+2	35	0.070	45.71	0.161	35	0.104	43.59	−0.365	35	0.809	25.84	−0.036	8 443	3 660
2805	1	38	0.938	24.01	0.628	38	0.375	38.11	−0.500	38	0.947	23.53	−0.058	14 003	6 646
2805	2	38	0.275	40.63	0.401	38	0.946	23.55	0.375	38	0.144	45.06	−0.185	14 106	6 629
2805	1+2	76	0.720	64.65	0.488	76	0.804	61.65	−0.200	76	0.593	68.59	−0.155	28 109	13 275
107	1	37	0.781	28.34	0.229	37	0.178	42.57	−0.239	37	0.001	181.14	−0.367	21 689	15 308
107	2	25	0.033	37.10	−0.193	25	0.499	22.38	0.174	25	0.010	41.87	2.024	16 257	11 962
107	1+2	62	0.235	65.44	−0.051	62	0.249	64.95	−0.104	62	0.001	223.01	−0.103	37 946	27 270
3007	1	9	0.354	8.88	−0.842	9	0.387	8.50	−0.618	9	0.117	12.87	−0.616	4 567	4 594
3007	2	10	0.892	4.30	−0.375	10	0.155	13.19	−0.473	10	0.198	12.29	1.138	4 326	4 063
3007	1+2	19	0.726	13.17	−0.760	19	0.198	21.69	−0.530	19	0.092	25.16	0.250	8 893	8 657

2409	1	17	0.023	27.99	−0.219	15	0.641	10.65	0.116	15	0.541	11.85	0.068	4 535	6 091
2409	2	21	0.680	15.68	0.058	20	0.180	23.32	−0.101	18	0.419	16.51	1.035	7 125	10 315
2409	1+2	38	0.125	43.67	−0.142	35	0.327	33.97	−0.050	33	0.500	28.35	0.608	11 660	16 406
501	1	29	0.320	29.89	0.626	30	0.887	19.39	−0.570	28	0.419	26.84	−0.363	18 807	17 603
501	2	22	0.023	34.61	−0.250	22	0.354	21.78	−0.083	22	0.196	25.16	−0.552	12 260	10 270
501	1+2	51	0.047	64.51	0.124	52	0.748	41.17	−0.294	50	0.253	52.01	−0.472	31 067	27 873
1401	1	63	0.667	51.92	0.093	62	0.499	55.40	−0.305	61	0.567	52.63	0.687	41 275	47 627
1401	2	63	0.755	49.35	−0.281	61	0.441	55.92	−0.167	59	0.282	58.49	1.007	34 019	33 801
1401	1+2	126	0.798	101.27	−0.079	123	0.475	111.32	−0.239	120	0.400	111.11	0.880	75 294	81 428
803	1	44	0.752	32.70	0.109	41	1.000	13.99	−0.619	40	0.844	26.67	0.512	36 169	47 563
803	2	44	0.982	22.96	0.636	40	0.244	40.43	0.266	38	0.600	30.37	−0.304	23 916	32 073
803	1+2	88	0.975	55.66	0.293	81	0.929	54.42	0.086	78	0.827	57.03	0.024	60 085	79 636
106	1	23	0.142	25.64	0.420	23	0.329	21.15	−0.600	23	0.410	19.76	−0.233	19 130	17 450
106	2	30	0.985	13.00	0.555	30	0.554	24.40	−0.628	29	0.136	32.84	−0.576	16 592	14 684
106	1+2	53	0.738	38.64	0.525	53	0.450	45.55	−0.623	52	0.176	52.60	−0.495	35 722	32 134
1307	1	30	0.494	27.47	0.445	26	0.233	28.70	−0.293	26	0.001	61.33	0.322	9 871	9 392
1307	2	28	0.960	14.88	1.682	22	0.471	19.80	−0.548	22	0.293	22.94	0.376	9 929	8 613
1307	1+2	58	0.876	42.35	0.825	48	0.297	48.50	−0.395	48	0.001	84.27	0.355	19 800	18 005
total	1	384	0.648	336.53	0.152	381	0.137	372.98	−0.185	370	0.001	507.68	−0.160	231 087	211 686
total	2	383	0.860	317.85	0.160	372	0.475	336.05	−0.315	362	0.048	368.89	0.147	196 533	169 054
total	1+2	767	0.852	654.38	0.075	753	0.207	709.03	−0.148	732	0.001	876.58	0.060	427 620	380 740

Total ($S35 + S36$): probability (χ^2) = 0.561; skewness = −0.016, pions = 808 360

1 – Date on the run.
2 – 1 (2) means $P > 0$ ($P > 0$).
3, 7, 11 – No. of measurements for each channel.
4, 8, 12 – Probability coming from the χ^2 analysis (the corresponding χ^2 values are reported in columns 5, 9, 13).
15 (16) – No. of pions counted in the channel S35 (S36).

so a very short time was needed for an accurate alignment. This fact allows us to interchange many times the two crystals during a run, and so to alternate the measurements of C_+ and C_-. This procedure results to be very useful in the measurements of small asymmetries.

3·2. – During the elaboration of the data a statistical analysis of the $C_\pm$ yields of the different eight channels has been done in order to check their internal consistence.

i) For each block of measurements those measurements with a deviation from the average $\bar{C}_+$ (or $\bar{C}_-$) larger than a limit value have been rejected. This limit value has been fixed on the basis of the number of independent measurements from which $\bar{C}_+$ (or $\bar{C}_-$) has been obtained.

Moreover, on the distribution of the accepted measurements a statistical analysis has been applied, by means of the « χ^2 test » and α (skewness)-test. A block of measurements has been rejected if its integral probability [$P(\chi^2)$ or $P(\alpha)$] was less than a given limit. Also this limit has been established on the basis of the independent measurements (see ref. [15]).

The statistical information obtained for each block of measurements has been combined, with a standard procedure, in order to obtain the confidence level of all the experiment.

The results for each run, as well as for all the experiment, are reported in Table II. For all the measurements we have obtained $P(\chi^2) = 0.56$, and $P(\alpha) = 0.62$ [corresponding to $\alpha = -0.016$].

ii) Finally, also to the calculated values of the asymmetry ratios $A(\theta, E_\gamma)$ a statistical analysis has been applied. For every angle θ we have rejected those results whose deviations from their best fit in E_γ (see [15]) exceeded a limit value ((2.3 ÷ 2.7) standard deviations), depending on the number of points of the fit. Thus we rejected three values of $A(\theta, E_\gamma)$ among 125 experimental points, *i.e.* a percentage of 2.4 %, in good agreement with the expected value (1.3 %).

3·3. – The most important contribution to the background, *i.e.* to the B_+ (or B_-), comes from processes originating from higher-energy photons, as the coherent bremsstrahlung beam extends until 1 GeV whereas the investigated interval producing single π^+ events is centered near to the « principal » maximum (see Fig. 3). Hence two backgrounds are present: i) π's, with the right momentum and angle, due to multipion processes, ii) muons from decay of higher-energy π's before or inside the magnet.

---

[15] For more details see: P. SPILLANTINI and V. VALENTE: Internal Report, LNF-67/61.

i) The « multipion background » has been measured or estimated in different ways:

a) We have measured the pion yield at a fixed kinematical condition (θ_l, p) for different values of the crystal's angle Θ, which means for different position (E_{peak}) of the « principal » maximum (Sect. 1).

This total yield is the superposition of a contribution of single-π^+ events which varies rapidly when the principal peak of the bremsstrahlung spectrum is made to « sweep » the energy band accepted by the experimental arrangement, and a slowly varying contribution of multipion processes originated in the high-energy region of the bremsstrahlung spectrum. In fact the number of photons whose energy is above the kinematical threshold for double (or multi-) production varies very slowly with the angle Θ.

Thus we may write for the pion's yield

$$(6) \qquad C_+(\Theta, \theta_l, p) = C_+ \text{ (single)} + C_+\text{(multipion)} =$$
$$= K\left\{ \int_{\Delta E_\gamma \Delta\Omega_l} N(\Theta, E_\gamma) \frac{\mathrm{d}\sigma_s(\theta_l, E_\gamma)}{\mathrm{d}\Omega_l} [1 + P(\Theta, E_\gamma) A(\theta_l, E_\gamma)] \cdot \right.$$
$$\left. \cdot G(E_\gamma)\, \mathrm{d}\Omega_l \mathrm{d}E_\gamma + B_+(\Theta, \theta_l, p) \right\}.$$

The quantities entering in (6) are:

$N(\Theta, E_\gamma)$: number of photons with energy E_γ when the crystal's angle is equal to Θ. This number is obtained from experimental spectra of the type reported in Fig. 3.

$\mathrm{d}\sigma_s/\mathrm{d}\Omega_l$: differential cross-section for unpolarized photons of energy E_γ to produce a pion in a single photoproduction process. For this cross-section we have used the results of ref. ([16]).

$G(E_\gamma)$: energy resolution function of the apparatus.

ΔE_γ, $\Delta\Omega_l$: energy band and solid angle accepted.

The quantities K, P, and A have been defined in Subsect. 3·1. The subscripts (+) refers to photons with polarization $P > 0$.

The multipion background $B(\Theta; \theta_l, p)$ is given by

$$(7) \qquad B(\Theta, \theta_l, p) = \int_{\Delta E_\pi \Delta\Omega_l} \int_{E_{\gamma th}}^{E_{\gamma max}} N(\Theta, E'_\gamma)\, \mathrm{d}E'_\gamma \frac{\mathrm{d}^2\sigma_p}{\mathrm{d}\Omega_l \mathrm{d}E_\pi} G(E'_\gamma)\, \mathrm{d}\Omega_l \mathrm{d}E_\pi ,$$

([16]) D. FREYTAG, W. J. SCHWILLE and R. J. WEDEMEYER: *Zeits. Phys.*, **186**, 1 (1965).

when ΔE_π is the spread in pion energy corresponding to ΔE_γ in (6) and $d^2\sigma_p/d\Omega_l\, dE_\pi$ is the differential cross-section by unpolarized photons of energy $E'_\gamma > E_{\gamma\,\text{threshold}}$, to produce in a multipion process a π^+ at (θ_l, p) (where p is the momentum corresponding to the energy E_π). We have assumed that this contribution is the same for both signs of beam polarization, as for $E_\gamma > E_{\gamma th}$ the polarization is very low.

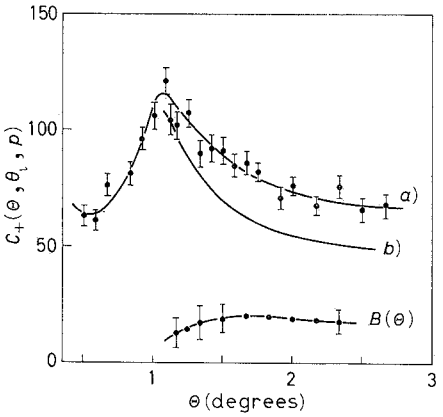

Fig. 10. – C_+ *vs.* Θ curve (see text Subsect. 3.2). $\theta_l = 30°$, $E_\pi = (284 \pm 15)$ MeV, $p = (239 \pm 16)$ MeV. *a*) Experimental, *b*) calculated.

By comparison of the experimental « C *vs.* Θ curve » with the theoretical one calculated from the first term of (6) it is possible to obtain $B(\Theta)$ (see Fig. 10)

As was expected, $B(\Theta)$ was found to be constant with Θ and its values for some typical kinematical conditions are summarized in Table III. In this Table the multipion background is expressed as percentage of the total pion yield for the various experimental conditions.

The measured values of B are in agreement with numerical calculation of (7) in which $d^2\sigma_p/d\Omega_l\, dE_\gamma$ is taken from the data of other laboratories ([17-19]).

TABLE III – B/C_+(single) + C_+(multipion).

θ	E_γ (MeV)		
	225	300	400
30°	0.50 ± 0.10	0.15 ± 0.10	0.45 ± 0.10
45°	0.23 ± 0.10	0.12 ± 0.04	0.30 ± 0.04
90°	0.05 ± 0.05	0.04 ± 0.05	0.16 ± 0.06

b) Direct measurements of multipion contribution due to the process

(8) $$\gamma + p \to p + \pi^+ + \pi^-$$

([17]) B. M. CHASAN, G. COCCONI, V. T. COCCONI, R. M. SCHECTMAN and D. H. WHITE: *Phys. Rev.*, **119**, 811 (1960).

([18]) M. BLOCH and M. SANDS: *Phys. Rev.*, **113**, 305 (1959).

([19]) A. KUSUMEGI, Y. KOBAYASHI, Y. MURATA, H. SASAKI, K. TAKAMATSU and A. MASAIKE: *Proceedings of the International Symposium on Electr. and Photon Interactions*, vol. 2 (Hamburg, 1965), p. 253.

have been performed revealing the π^- in the same kinematical condition as for π^+ in single photoproduction process and with the same coherent beam spectrum, only reversing the current in the magnetic spectrometer.

From such measurements we have estimated the total multipion background, including the process

$$\gamma + p \to n + \pi^+ + \pi^0 , \tag{8'}$$

making use of the experimental data of BLOCH and SAND [18] and of KUSUMEGI *et al.* [19] to fix the relative weight of the two processes.

Also these calculations agree with the results of Table III.

ii) Besides the multipion background now discussed we have also some losses in the pion's counting rate due to the $(\pi \to \mu)$ decay of pions of right momentum along their trajectories. As this loss is equal, for the two cases $(P \gtrless 0)$, *i.e.* of the type $B_+/C_+ = B_-/C_-$, it can be ignored, in the calculation of the asymmetry A (see (7)). Moreover, because of the momentum discontinuity at the decay, we have contamination also from parent π's with a momentum outside our accepted band. A part of this contamination is contained in the multipion subtraction just discussed.

Finally, some other minor backgrounds (like empty target (*)) are also of the type $B_+/C_+ = B_-/C_-$ and, therefore, have been ignored in the calculation of A.

4. – Experimental results.

With the technique and the procedure described in the preceding paragraphs we have measured the asymmetry ratios $A(\theta, E_\gamma)$, for $\theta = 30°$, 45°, 71°, 90°, 120°, 133°, 144° and $E_\gamma = (200 \div 450)$ MeV, reported in Fig. 11 and Table IV.

As we have explicitly shown in [8] (see Fig. 1 in [8]) many measurements of $A(\theta, E_\gamma)$ have been repeated with different values of beam polarization P and were found to be completely consistent.

The errors of the asymmetry ratios A have been calculated by means of the following expression:

$$\Delta A = \frac{2}{P}\frac{R}{(R+1)^2}\left\{\left(\frac{\Delta C_+}{C_+ - B}\right)^2 + \left(\frac{\Delta C_-}{C_- - B}\right)^2 + h^2\left(\frac{\Delta B}{B}\right)^2 + A^2\left(\frac{\Delta P}{P}\right)^2\right\}^{\frac{1}{2}}, \tag{9}$$

(*) The empty-target contribution has been measured for different kinematical conditions and resulted to be less than 5%.

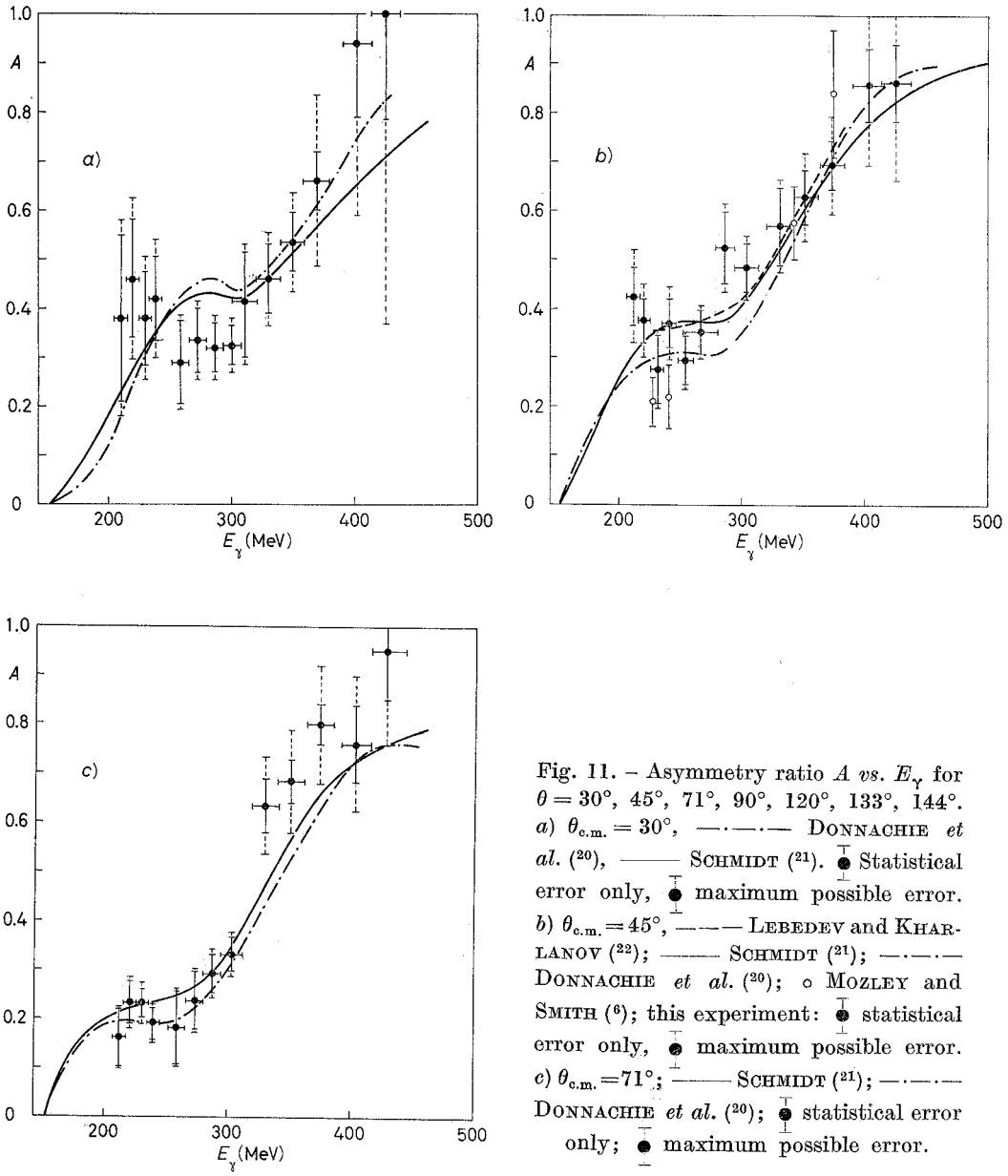

Fig. 11. – Asymmetry ratio A *vs.* E_γ for $\theta = 30°$, 45°, 71°, 90°, 120°, 133°, 144°. *a*) $\theta_{c.m.} = 30°$, —·—·— DONNACHIE *et al.* ([20]), ——— SCHMIDT ([21]). ⊕ Statistical error only, ⊕ maximum possible error. *b*) $\theta_{c.m.} = 45°$, ——— LEBEDEV and KHARLANOV ([22]); ——— SCHMIDT ([21]); —·—·— DONNACHIE *et al.* ([20]); ○ MOZLEY and SMITH ([6]); this experiment: ⊕ statistical error only, ⊕ maximum possible error. *c*) $\theta_{c.m.} = 71°$; ——— SCHMIDT ([21]); —·—·— DONNACHIE *et al.* ([20]); ⊕ statistical error only; ⊕ maximum possible error.

([20]) A. DONNACHIE, F. A. BERENDS and D. L. WEAVER: CERN, preprint TH. 744, February 1967.

([21]) W. SCHMIDT: private communication.

([22]) A. J. LEBEDEV and S. P. KHARLANOV: Phys. Inst. P. P. Lebedev Internal report n. 69 (1967).

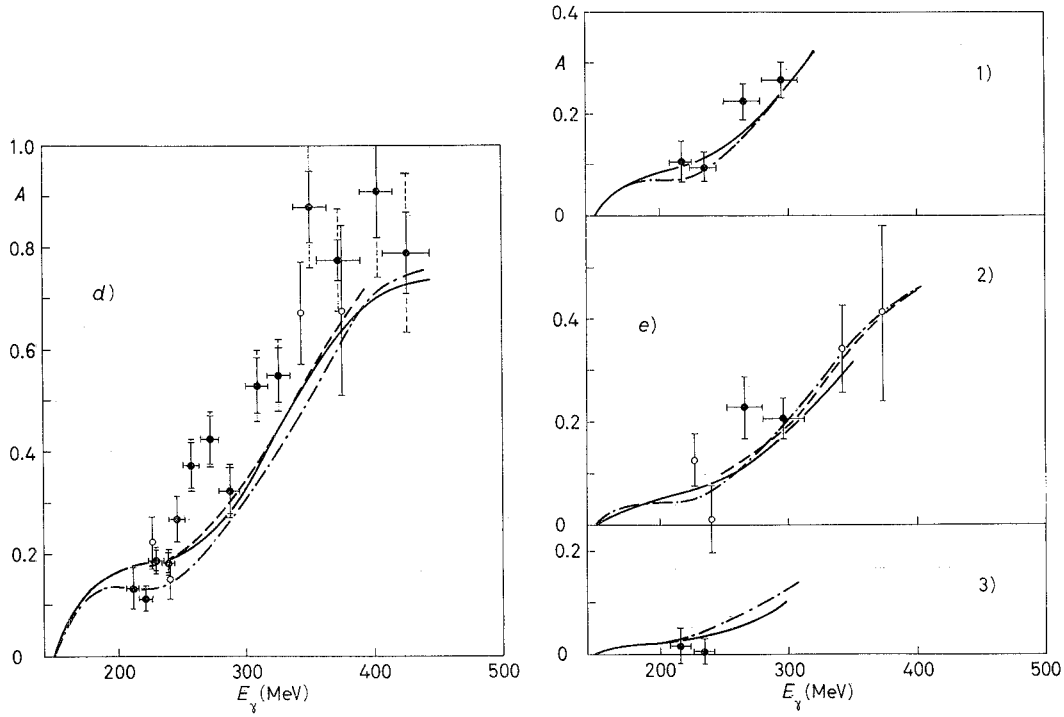

Fig. 11. – Asymmetry ratio A *vs.* E_γ for $\theta = 30°$, 45°, 71°, 90°, 120°, 133°, 144°. *d*) $\theta_{c.m.} = 90°$; ——— SCHMIDT [21]; —·—·— DONNACHIE *et al.* [20]; ——— LEBEDEV and KHARLANOV [22]; ○ MOZLEY and SMITH; this experiment: ⊕ statistical error only; ⊕ maximum possible error. *e*) —·—·— DONNACHIE *et al.* [20]; ——— SCHMIDT [21]; ——— LEBEDEV and KHARLAMOV [22]; ○ MOZLEY and SMITH; • this experiment. 1) $\theta_{c.m.} = 120°$, 2) $\theta_{c.m.} = 133°$, 3) $\theta_{c.m.} = 144°$.

where

$$R = \frac{C_+ - B}{C_- - B} \qquad \text{and} \qquad h = \frac{(C_+ - C_-)/B}{(C_+ \times C_-)/B^2 - (C_+ - C_-)/\mathrm{B} + 1}\,.$$

The first two terms in (9) are the statistical errors of the yields C_+ and C_-, whereas the third and fourth terms are, respectively, the relative error on the background B and on the beam polarization P.

The statistical errors in our experiment were $\sim (1 \div 2)\,\%$ ($C_+ \sim C_- \geqslant 10\,000$). The error in the beam polarization was estimated to be $\Delta P/P \sim 2\,\%$, so the term $A \cdot (\Delta P/P)$ gives a contribution to ΔA of the same order of the statistical error.

The precision in the multipion background (see Table III in 3·2) is, generally, worse. But, the contribution of this background subtraction in ΔA

TABLE IV.

$\theta_{c.m.}$	E_γ	A	ΔA (*)	ΔA (**)
30°	211 ± 5	0.380	0.199	0.168
	220 ± 5	0.459	0.167	0.121
	230 ± 5	0.381	0.126	0.096
	239 ± 5	0.422	0.118	0.086
	259 ± 7	0.289	0.097	0.086
	273 ± 7	0.334	0.081	0.066
	287 ± 7	0.318	0.064	0.048
	301 ± 7	0.323	0.057	0.039
	311 ± 10	0.414	0.114	0.099
	330 ± 10	0.458	0.094	0.071
	350 ± 11	0.536	0.097	0.057
	370 ± 11	0.663	0.175	0.058
	402 ± 12	0.940	0.349	0.148
	425 ± 12	1.000	0.637	0.213
45°	211 ± 5	0.427	0.094	0.061
	220 ± 5	0.373	0.077	0.046
	230 ± 5	0.273	0.082	0.071
	240 ± 6	0.372	0.074	0.051
	254 ± 6	0.293	0.060	0.050
	267 ± 13	0.353	0.056	0.047
	285 ± 8	0.525	0.088	0.075
	303 ± 10	0.487	0.064	0.048
	330 ± 10	0.568	0.098	0.081
	351 ± 10	0.629	0.091	0.056
	372 ± 10	0.693	0.105	0.052
	403 ± 13	0.859	0.166	0.075
	428 ± 12	0.866	0.199	0.081
71°	211 ± 5	0.158	0.062	0.059
	220 ± 5	0.231	0.052	0.043
	230 ± 5	0.231	0.042	0.030
	239 ± 5	0.190	0.036	0.028
	258 ± 7	0.180	0.079	0.077
	273 ± 7	0.235	0.066	0.062
	287 ± 7	0.291	0.048	0.038
	303 ± 9	0.331	0.046	0.033
	330 ± 11	0.635	0.102	0.055
	351 ± 11	0.686	0.105	0.044
	373 ± 11	0.791	0.117	0.036
	402 ± 12	0.761	0.141	0.079
	427 ± 12	0.952	0.198	0.098

(*) Maximum possible error (see text).
(**) Statistical error.

TABLE IV (*continued*).

$\theta_{c.m.}$	E_γ	A	ΔA (*)	ΔA (**)
90°	211 ± 5	0.136	0.040	0.039
	221 ± 5	0.117	0.026	0.025
	229 ± 6	0.192	0.026	0.022
	239 ± 5	0.183	0.025	0.022
	246 ± 6	0.270	0.046	0.043
	257 ± 6	0.376	0.050	0.045
	272 ± 7	0.425	0.052	0.048
	287 ± 8	0.326	0.048	0.043
	309 ± 9	0.530	0.068	0.055
	326 ± 9	0.552	0.068	0.055
	351 ± 13	0.879	0.118	0.071
	373 ± 17	0.775	0.101	0.040
	403 ± 13	0.911	0.163	0.088
	426 ± 19	0.791	0.156	0.079
120°	217 ± 8	0.105	0.041	0.041
	235 ± 10	0.095	0.027	0.027
	265 ± 15	0.231	0.035	0.033
	295 ± 15	0.261	0.030	0.028
133°	265 ± 15	0.215	0.063	0.062
	296 ± 16	0.204	0.043	0.042
144°	217 ± 8	0.016	0.037	0.037
	235 ± 10	0.002	0.026	0.025

is depressed, by the coefficient h which is, generally, much less than unity.

In Fig. 11 and in Table IV we report, separately, for ΔA the statistical error and the maximum possible error, calculated by including all the terms in (9).

Only for comparison we report in Fig. 11 also the predictions of the more recent theories ([20-22]).

A short discussion of these results has been reported at Dubna Conference ([23]) and in ([5,24]).

A full discussion of these data in comparison with the theoretical predictions will be done later.

([23]) M. GRILLI, M. NIGRO, E. SCHIAVUTA, F. SOSO, P. SPILLANTINI and V. VALENTE: *Recent measurements of π^+ photoproduction with coherent bremsstrahlung ($E_\gamma = (200 \div 450)$ MeV)*, internal report LNF-67/18; *Communication of the International Conference on Electromagnetic Interactions at Low and Intermediate Energies, Dubna, February* 7-15, 1967.

([24]) M. GRILLI, M. NIGRO and E. SCHIAVUTA: *Nuovo Cimento*, **49**, 326 (1967).

RIASSUNTO

Nel presente lavoro sono descritti l'apparecchiatura ed il metodo sperimentale usati in una serie di misure della fotoproduzione singola di π^+ con γ linearmente polarizzati. Si riportano i risultati ottenuti per il rapporto di asimmetria $A(\theta)$ nell'intervallo $\theta = (30 \div 145)°$ (c.m.) e per $E_\gamma = (200 \div 450)$ MeV.

Фоторождение положительных пионов линейно поляризованными γ-лучами.
I. - Экспериментальный метод и результаты.

Резюме (*). — Описываются аппаратура и экспериментальный метод, использованные для измерений фоторождения одного π^+ линейно поляризованными γ-лучами. Приводятся результаты для асимметричного отношения $A(\theta)$. Наши результаты покрывают область $\theta = (30 \div 145)°$ (Ц.М.) и $E_\gamma = (200 \div 450)$ МэВ.

(*) *Переведено редакцией.*

M. GRILLI, *et al.*
21 Aprile 1968
Il Nuovo Cimento
Serie X, Vol. **54** A, pag. 877-896